Nicotine Inhibits Amyloid Formation by the β-Peptide†

Arthur R. Salomon,‡ Keith J. Marcinowski,‡ Robert P. Friedland,§ and Michael G. Zagorski*,‡

Department of Chemistry and Department of Neurology, School of Medicine, Case Western Reserve University, Cleveland, Ohio 44106

Received July 15, 1996⊗

ABSTRACT: The 42-residue β-(1−42) peptide is the major protein component of amyloid plaque cores in Alzheimer's disease. In aqueous solution at physiological pH, the synthetic β-(1−42) peptide readily aggregates and precipitates as oligomeric β-sheet structures, a process that occurs during amyloid formation in Alzheimer's disease. Using circular dichroism (CD) and ultraviolet spectroscopic techniques, we show that nicotine, a major component in cigarette smoke, inhibits amyloid formation by the β-(1−42) peptide. The related compound cotinine, the major metabolite of nicotine in humans, also slows down amyloid formation, but to a lesser extent than nicotine. In contrast, control substances pyridine and *N*-methylpyrrolidine accelerate the aggregation process. Nuclear magnetic resonance (NMR) studies demonstrate that nicotine binds to the 1−28 peptide region when folded in an α-helical conformation. On the basis of chemical shift data, the binding primarily involves the N-CH_3 and 5′CH_2 pyrrolidine moieties of nicotine and the histidine residues of the peptide. The binding is in fast exchange, as shown by single averaged NMR peaks and the lack of nuclear Overhauser enhancement data between nicotine and the peptide in two-dimensional NOESY spectra. A mechanism is proposed, whereby nicotine retards amyloidosis by preventing an α-helix → β-sheet conformational transformation that is important in the pathogenesis of Alzheimer's disease.

The brains of patients with Alzheimer's disease (AD) contain an abundance of amyloid plaques containing the β-peptide [for recent reviews, see Iversen et al. (1995) and Selkoe (1994)], which is a small peptide composed of 39−42 amino acid residues (Figure 1). The β-peptide is a normal, soluble physiological component (Gravina et al., 1995). However, under certain environmental conditions, the β-peptide can produce oligomeric β-sheet structures that eventually precipitate as amyloid plaques (Kirschner et al., 1987; Gorévic et al., 1987; Hilbich et al., 1991; Barrow & Zagorski, 1991; Burdick et al., 1992; Terzi et al., 1994). The soluble β-sheet structure has the following properties that are relevant to amyloidosis in AD: (1) it is a precursor to the insoluble β-pleated sheet structure in amyloid plaque, (2) it can act as a seed that nucleates amyloid formation (Jarrett & Lansbury, 1993; Snyder et al., 1994), and (3) it is neurotoxic to hippocampal neuronal cultures (Simmons et al., 1994; Harrigan et al., 1995; Pike et al., 1995). For these reasons, a major goal of research is now focused on identifying substances that prevent β-sheet formation and the accompanying precipitation of β-peptide into amyloid. Despite the numerous substances known to enhance amyloidosis, relatively few are known to inhibit it [for examples, see Eriksson et al. (1995), Janciauskiene et al. (1995), and Wood et al. (1996)], particularly in a conformationally specific manner.

A major focus of our research is to provide a molecular basis for amyloid formation in AD. The recent reports of an inverse relationship between the risk of AD and cigarette smoking (Graves et al., 1991; Van Duijn & Hofman, 1991; Brenner et al., 1993; Friedland, 1994; Graves & Mortimer, 1994), together with the ability of nicotine to be neuroprotective and inhibit β-peptide cytotoxicity (Shimohama, 1996; Kihara et al., 1996), inspired us to investigate the effects of nicotine and cotinine on the solution conformations and aggregational properties of the β-peptide. Nicotine is a major component of cigarette smoke that is metabolized and excreted as cotinine. We report here that nicotine prevents the synthetic β-(1−42) peptide from precipitating as an amyloid-like deposit. The CD and NMR spectroscopic data suggest that the inhibition may result from the binding of nicotine to the more soluble α-helical structure, which in turn impedes an α-helix → β-sheet (soluble) → β-sheet (precipitate) process from occurring.

MATERIALS AND METHODS

Sample Preparation. The pH values were measured with a pH meter (Model PHB-62, Omega Engineering, Inc.) equipped with an electrode (Model MI-412, Microelectrodes, Inc.) that was calibrated with pH 4.00 and 7.00 buffers. Unless specified otherwise, all peptide solutions were prepared in 14 mM sodium phosphate buffer at pH 7.2. Distilled and deionized water, nicotine, cotinine, pyridine, and *N*-methylpyrrolidine were of the highest grade possible from commercial sources and were used without further purification. The β-(1−28) peptide was synthesized, purified, and characterized as described previously (Barrow et al., 1992), while the β-(1−42) peptide was purchased in crude form from Anaspec, Inc., and purified by high-performance liquid chromatography (HPLC) in our laboratory. Analysis of the HPLC-purified peptides by proton (^{1}H)

† Supported in part by Philip Morris, U.S.A. (R.P.F.), the American Health Assistance Foundation (M.G.Z.), the Suntory Institute for Bioorganic Research (M.G.Z.), and a Faculty Scholars Award, Alzheimer's Association (M.G.Z.). The 600 MHz NMR spectrometer was purchased with funds provided by the National Science Foundation, the National Institutes of Health, and the State of Ohio.

* Author to whom correspondence should be addressed: telephone, (216) 368-3706; Fax, (216) 368-3006; E-mail, mxz12@po.cwru.edu.

‡ Department of Chemistry.

§ Department of Neurology, School of Medicine.

⊗ Abstract published in *Advance ACS Abstracts,* October 1, 1996.

S0006-2960(96)01726-6 CCC: $12.00

NMR spectroscopy in deuterated trifluoroacetic acid solvent showed that they were approximately 95% pure.

A major difficulty with solution studies of the β-(1−42) peptide relates to the ease in which it aggregates and precipitates. It has been established that the soluble β-sheet structure of the β-(1−42) peptide is neurotoxic (Simmons et al., 1994; Harrigan et al., 1995; Pike et al., 1995); however, there still exists some discrepancy about the levels of neurotoxicity [for a review, see *Neurobiology of Aging* (1992) 13, 535−623; Wujek et al., 1996]. In fact, several groups have reported that synthetic β-peptides show either trophic or toxic responses on neurons in vitro. Although the reasons for these deviations are unknown, they are believed to arise in part from differences in the aggregation states and the solution structures of the β-peptides. The ability to produce the presumably neurotoxic, aggregated β-sheet structure is dependent on many factors, particularly the peptide concentration, ionic strength, and solvent polarity (Barrow & Zagorski, 1991; Barrow et al., 1992; Hilbich et al., 1991; Shen et al., 1994; Snyder et al., 1994). For example, the aggregation rate is extremely rapid in aqueous acetonitrile solutions, such as those used for HPLC purification of the peptide (Shen & Murphy, 1995). The longer that the β-(1−42) peptide remains in aqueous acetonitrile solution, the more likely it will become an aggregated β-sheet structure. Additionally, different commercially prepared batches of HPLC-purified β-(1−42) peptides can have different starting aggregation states and structures (Soto et al., 1995b), which will then in turn affect their solubility, aggregation rates, biological activities in solution (Busciglio et al., 1992, Pike et al., 1993, Simmons et al., 1994, Wujek et al., 1996), and the ability to reproduce biophysical measurements.

To partly overcome the above complications, we developed a pretreatment method that involves sonicating the dry peptide in concentrated trifluoroacetic acid (TFA) before biophysical measurements. The TFA breaks up the preaggregated peptides and affords monomeric random coil structures. This method ensures that different batches of purified β-(1−42) peptide will provide reproducible starting points for biophysical and neurotoxicity studies. A more complete description of this pretreatment method will be presented in a forthcoming paper.

Circular Dichroism Measurements and Data Analysis. All CD spectra were obtained at room temperature with a Jasco spectropolarimeter (Model J-600A). A quartz cell (Hellma, Inc.) of 1 mm path length was used to obtain spectra at 1 nm intervals from 190 to 260 nm. Spectra resulted from averaging four scans, followed by subtraction of the CD spectrum for phosphate buffer with or without nicotine. For studies following the variations of secondary structure over time, the first spectrum (time 0 h) was taken 30 min after peptide dissolution while subsequent spectra were taken at time intervals relative to time 0 h. The data were analyzed with the Jasco J-600 program that was located on the DP-501 computer of the spectropolarimeter or off-line on a Macintosh Power PC-7100 computer.

The β-(1−42) peptide adopts 100% oligomeric β-sheet structure in solution before it precipitates as an amyloid-like, oligomeric β-pleated sheet structure (Kirschner et al., 1987; Barrow et al., 1992). Once the precipitation starts, the solution conformation will remain 100% β-sheet and the ellipticities will decrease in amplitude since the peptide concentration in solution decreases. In general, the determination of the secondary structure of peptides and proteins from CD spectra usually employs equations that compare the observed and the expected maximum mean-residue ellipiticities ($[\theta]\tau$) at a specific wavelength (τ) that is characteristic for a particular secondary structure. The β-sheet structure is characterized by a maximum at 195 nm and a minimum at 217 nm (Greenfield & Fasman, 1969). If a peptide folds into 100% β-sheet, then the experimentally observed $[\theta]_{217}$ should be −18 400 deg·cm^2/dmol. However, the determination of the $[\theta]\tau$ value is critically dependent upon both the measured ellipticity $(\theta)\tau$ and an accurate peptide concentration. The present study followed CD spectra of the β-(1−42) peptide over time, in which the peptide concentrations changed. This indicated that an alternative procedure was needed to estimate the amount of soluble β-sheet structure. The method we used compared spectra recorded at different times, and the percent soluble β-sheet structure was obtained by comparing the ratio between the ellipticities at 195 and 217 nm. The ratio where precipitation started was standardized to 100% β-sheet. Similar procedures have been utilized to obtain reliable estimates of secondary structures for other peptides [see Muñoz et al. (1995) and references cited therein].

Precipitation Assay Using Ultraviolet Spectroscopy. The β-(1−42) peptide (0.73 mg, 0.15 μmol) was dissolved in 0.1 mL of a 5% aqueous TFA solution. The solution was adjusted to pH 1.5 by adding microliter amounts of neat TFA and then sonicated for 60 min, followed by dilution to a final volume of 3.0 mL with the addition of a pH 7.2 phosphate buffer solution (14 mM). The β-(1−42) concentration was now 50 μM. Because the aggregational properties of the peptide rapidly increase below pH 7 (Fraser et al., 1991; Barrow & Zagorski, 1991; Burdick et al., 1992), the pH of the final solution was always immediately checked to ensure that it was above 7.1. In most cases, the pH remained at 7.2, indicating that a 14 mM phosphate buffer concentration was adequate to maintain the pH. However, if the pH was less than 7, it was then quickly raised to pH 7.2 by the addition of microliter amounts of dilute potassium hydroxide solution. After ensuring the pH was properly adjusted, the solution was split equally into two 1.5 mL fractions. To one fraction was added an aliquot (2.4 μL) of a 15 mM aqueous solution of (*S*)-(−)-nicotine in phosphate buffer (14 mM, pH 7.2). No corrections of pH readings were made after the addition of the nicotine since control experiments showed that this addition did not alter the pH. Similar procedures were employed for the studies with cotinine, pyridine, and *N*-methylpyrrolidine, in which 15 mM stock solutions of these substances were prepared in aqueous phosphate buffers and then added to the peptide solutions.

The two fractions were centrifuged at 3800 rpm for 1 h each day immediately preceding the UV measurement. Aliquots of the resulting supernatants were assayed for absorbance at 210 nm with a Perkin-Elmer Lambda 3B UV/vis spectrophotometer. The absorbance value obtained for the nicotine−peptide solution was compared to the absorbance of the peptide in buffer alone, and the values obtained were expressed as percent soluble peptide.

Nuclear Magnetic Resonance Spectroscopy. All ^{1}H NMR spectra were obtained at 270 or 600 MHz using Bruker AC-270 or Varian UnityPlus-600 spectrometers. The NMR data was transferred to Indigo-XS24-R4000 (Silicon Graphics, Inc.) computer workstations and processed using the FELIX

program (version 2.3, Biosym, Inc.). The NMR solutions were prepared in deuterated water (D_2O) solution (0.6 mL) with sodium phosphate buffer (14 mM, pH 7.2), perdeuterated sodium dodecyl sulfate (SDS-d_{25}) (10 or 20 mM), perdeuterated ethylenediaminetetraacetic acid (Na_2EDTA-d_{12}, 0.5 mM), NaN_3 (0.05 mM), and 3-(trimethylsilyl)-propionate-2,2,3,3-d_4 (TSP) (0.05 mM), the latter serving as an internal chemical shift reference at 0 ppm. The Na_2-EDTA, D_2O, and SDS-d_{25} were purchased from Isotec, Inc., and Cambridge Isotopes, Inc. To ensure that the phosphate buffer maintained pH 7.2, the pH of the final solutions was always checked with a special pH electrode (Microelectrodes, Inc.) that fit inside the 5 mm NMR tube. In all cases, the buffer maintained pH 7.2, so no further adjustments of the pH were needed. No corrections of pH readings for deuterium isotope effects or for the presence of the SDS-d_{25} were performed, since control experiments showed that these substances did not significantly alter the pH.

The NMR measurements were performed at 30.0 °C, and the carrier was placed in the center of the spectrum at the position of the residual protium absorption of D_2O (HDO). The HDO signal was suppressed by low-power irradiation during the recycle delay. For one-dimensional (1D) spectra, 128 scans were acquired with a total recycle delay of 4.2 s, which included an acquisition time and recycle delay of 2.2 and 2.0 s, respectively The digital resolution of the acquired data was 0.24 Hz/point, which was reduced to 0.12 Hz/point by zero-filling the data once before processing. To further improve the resolution, before Fourier transformation spectra were multiplied by a Lorentzian-to-Gaussian weighting factor.

The majority of the ^{1}H NMR peaks of the β-(1−28) peptide in aqueous SDS-d_{25} solution were assigned and briefly described by us in an earlier publication (Talafous et al., 1994). The ^{1}H NMR peaks of nicotine in D_2O containing 20 mM SDS-d_{25} were assigned at 30.0 °C using a standard absolute value two-dimensional (2D) COSY spectrum (Wüthrich, 1986). The 2D NOESY data (Kumar et al., 1980) for nicotine, the β-(1−28) peptide, and a 2:1 mixture of nicotine−β-(1−28) were acquired in the phase-sensitive mode with quadrature detection in both dimensions (States et al., 1982). The irradiation was carried out during both the recycle delay (1.5 s) and the mixing time (250 ms). Before Fourier transformation spectra were multiplied by a skewed sine-bell-squared window function in F_2 and a 90° phase-shifted sine bell in F_1. Baseline roll was reduced by careful adjustment of the intensity of the first points in F_2 and F_1 (Otting et al., 1986) and by the application of a cubic-polynomial baseline correction of the rows in the final 2D matrix. For the data acquired at 600 MHz, the spectral width in both dimensions was 7000.4 Hz, and 256 complex increments (each consisting of 40 scans) were acquired with 2048 points for the F_2 dimension. The data were zero-filled twice in the F_1 dimension to provide 2D matrices consisting of 1024 × 1024 points.

RESULTS

Shown in Figure 1 are the primary sequences of the two synthetic β-peptides used in the present study. These are the β-(1−28) and β-(1−42) peptides that contain residues 1−28 and 1−42 of the amyloid β-peptide. Among the various sized β-peptides, the 42-residue β-(1−42) peptide

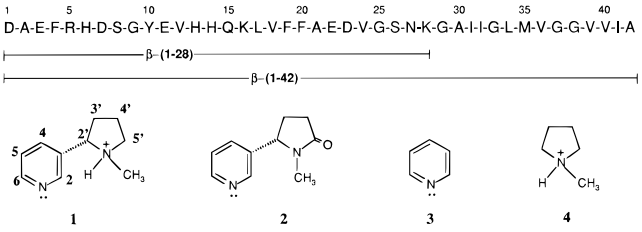

FIGURE 1: Amino acid sequences for the amyloid β-(1−28) and β-(1−42) peptides, together with the chemical structures of (*S*)-(−)-nicotine (**1**), (*S*)-(−)-cotinine (**2**), pyridine (**3**), and *N*-methylpyrrolidine (**4**). The protonation states for the nitrogens are in accordance to the major species that exists at pH 7.2.

is the most insoluble and can act as a seed that nucleates amyloid formation (Jarrett & Lansbury, 1993; Snyder et al., 1994; Tamaoka et al., 1994). The β-(1−42) peptide is the predominant protein component in cerebrovascular amyloid and plaque core deposits (Roher et al., 1993; Gravina et al., 1995), and familial AD amino acid substitutions of the amyloid precursor protein favor production of the longer β-(1−42) over the shorter β-(1−40) peptide (Suzuki et al., 1994). Because these results implicate the β-(1−42) peptide in the development of amyloid plaques, we chose to study it in our CD and precipitation studies. As described in the Materials and Methods section, our protocol ensured that the peptide was in a well-defined, monomeric state before starting the CD and precipitation assays.

The chemical structures of nicotine (**1**), cotinine (**2**), pyridine (**3**), and *N*-methylpyrrolidine (**4**) are also shown in Figure 1. The biologically active stereoisomers of **1** and **2**, which are (*S*)-(−)-nicotine and (*S*)-(−)-cotinine, related to cigarette smoke were used in the present study. The nicotine structure shown in Figure 1 represents the predominant species at physiological pH, in which the *N*-methylpyrrolidine nitrogen is protonated (pK_a 8.02) and the pyridine nitrogen is not protonated (pK_a 3.12) (Lide, 1991). The pyrrolidine nitrogen in cotinine is part of an amide bond with the neighboring carbonyl and therefore is not protonated at physiological pH. The structurally related compounds, pyridine and *N*-methylpyrrolidine, were used as control substances, as these compounds are also heterocyclic amines and represent distinct subregions of nicotine (Figure 1). The pK_a values for pyridine and N-methylpyrrolidine are 5.25 and 11.27 (Lide, 1991), so that at pH 7.2 the protonation state of the nitrogens is similar to nicotine.

Effect of Nicotine on the Rate of β-Sheet Formation. The CD spectra for two solutions containing identical quantities of 50 μM monomeric β-(1−42) peptide are shown in Figure 2A,B. Both solutions were prepared in aqueous 14 mM phosphate buffer, and one of the solutions also contained 1 molar equiv of nicotine (Figure 2B). A 50 μM β-(1−42) peptide concentration was selected since subtle conformational changes as well as the aggregation rates can be conveniently monitored by CD. Peptide concentrations above 50 μM underwent very rapid conformational change and aggregated too quickly to be monitored by CD, while lower peptide concentrations are too stable and require other components to promote aggregation (Iversen et al., 1995).

The changes in secondary structure were monitored by recording CD spectra at different time intervals (Figure 2A,B). The time 0 h corresponds to CD spectra taken 20 min after peptide dissolution, while the remaining spectra were taken 24, 48, 72, 96, and 120 h later. For the control

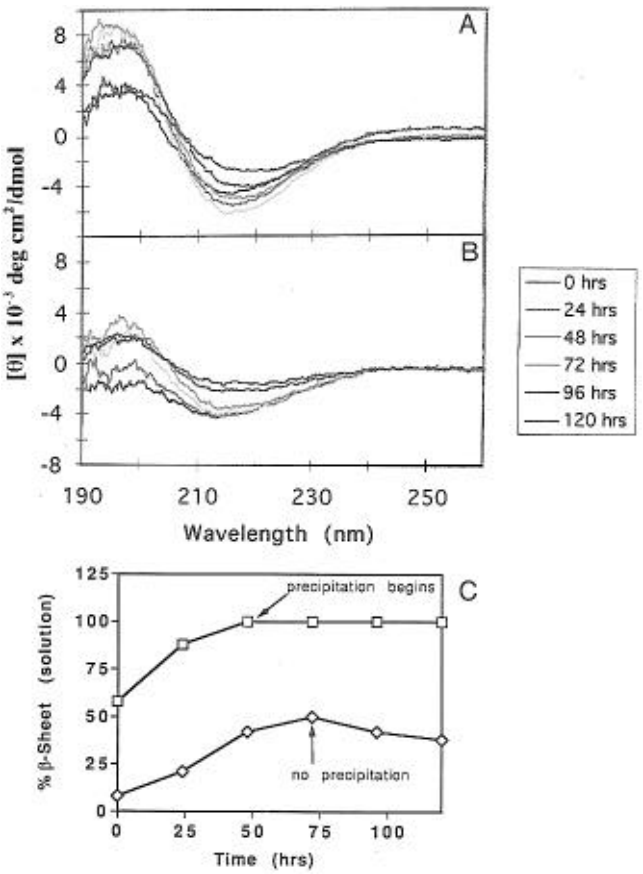

FIGURE 2: CD spectra for a 50 μM solution of monomeric β-(1−42) peptide alone (upper, A) and for an identical peptide solution containing 50 μM nicotine (lower, B). For clarity, the overlaid traces are shown in color and correspond to spectra obtained at 0, 24, 48, 72, 96, and 120 h of incubation at room temperature. The CD traces for time 0 were recorded approximately 30 min after peptide dissolution. The lower trace (C) is a graph showing the percent β-sheet structure as determined from the CD spectra (A and B), with the open rectangles corresponding to the upper (A) spectra without nicotine and the diamonds representing the lower (B) spectra with nicotine. As shown, at time 0 the solution without nicotine produces 58% β-sheet structure, which begins to precipitate after 48 h. This high initial content of β-sheet structure occurs during the 30 min interval involved with dissolving the monomeric, random coil peptide and then recording the CD spectrum.

peptide solution without nicotine (Figure 2A), at 24, 48, 72, 96, and 120 h there is a mixture of only two conformations, β-sheet and random coil. This conclusion is supported by the presence of an isodichroic point at 205 nm, in which the ellipticity (θ) intensities are equal. In contrast, for the solution with nicotine (Figure 2B) no isodichroic point is apparent, suggesting that greater than two conformations exist in solution.

The percent soluble β-sheet structure at each time interval was determined, and the results are shown graphically in Figure 2C. The β-sheet conformation is characterized by a positive band at 195−197 nm and a broad negative band at 214−217 nm (Greenfield & Fasman, 1969; Woody, 1994). Initially, at 0 h there is 8% and 58% β-sheet structure for the solutions with and without nicotine, respectively. The β-sheet structure is oligomeric and forms immediately in water solution, particularly at β-(1−42) peptide concentrations greater than 10 μM (Barrow et al., 1992). At subsequent time intervals, the [θ] for the CD bands centered at 196 and 215 nm get stronger, corresponding to increases in the amount of soluble β-sheet structure. For the control peptide solution, the soluble β-sheet content increases to 88% and 100% at 24 and 48 h, but then at 72, 96, and 120 h the peptide begins to precipitate, causing the CD bands at 196 and 215 nm to get weaker θ values. Although for these latter times the θ values are weaker, the amount of soluble β-sheet remains 100% (Figure 2C). In previous work we showed that the β-(1−42) peptide adopts 100% oligomeric β-sheet structure in solution immediately before it precipitates as an amyloid-like oligomeric β-pleated sheet structure (Barrow et al., 1992). The precipitation decreases the peptide concentration in solution, but the overall (solution and precipitate) β-sheet content remains 100%.

For the peptide solution containing nicotine, the soluble β-sheet content rises to a maximum of 50% at 72 h and then drops to 40% and 38% for the remaining time. Most significantly, no peptide precipitation was detected for this solution. These data establish that nicotine causes a reduction in the kinetics of β-sheet formation and an accompanying loss of the precipitation.

Effect of Nicotine on the Rate of β-(1−42) Precipitation. To ascertain the effects of nicotine on the rate of β-(1−42) precipitation, we performed separate studies using centrifugation and ultraviolet spectroscopy. These techniques have been successfully applied to related precipitation studies with the amyloid β-peptides (Brunden et al., 1993; Bush et al., 1994). The recently reported problems (Esler et al., 1996) in using ultraviolet spectroscopy for quantification of very dilute β-peptide samples is not pertinent, since much higher peptide concentrations were used in the present study.

Two peptide solutions [50 μM β-(1−42), 14 mM phosphate buffer, pH 7.2] were analyzed at 24-h intervals over 5 days. One of the solutions contained 1 molar equiv of nicotine. For each interval, the supernatant after centrifugation was inspected by ultraviolet spectroscopy to determine the amount of soluble β-(1−42) peptide, and a graph displaying the results is shown in Figure 3A. The amount of soluble β-(1−42) peptide for the control solution without nicotine rapidly declines, 98% → 78% → 69% → 51% for the first 3 days, and then falls to 40% and 33% at days 4 and 5. The solution containing nicotine shows no precipitation for the first 3 days and only a slight 4−5% reduction in soluble β-(1−42) peptide at days 4 and 5. The inhibition to precipitation could be reproduced three times, and analysis of the data from the three different experiments indicate that our measurements are accurate to ±10%. Error bars reflecting the ±10% are included in the graphs of Figure 3.

At lower concentrations, using a β-(1−42) solution at 3.1 μM, precipitation of the control peptide solution was noticed after 3 days, whereas for an identical 3.1 μM peptide solution containing 1 molar equiv of nicotine no precipitation was detected up to 7 days. The peptide concentration of 3.1 μM was the lowest concentration in which reliable detection by ultraviolet spectroscopy could be seen without interfering background interference.

Another precipitation study was performed to examine the effects of control substances on the rate of precipitation of the β-(1−42) peptide. This study used nicotine (**1**), cotinine (**2**), pyridine (**3**), and *N*-methylpyrrolidine (**4**) (Figure 1). The percent soluble β-(1−42) peptide, with four solutions containing 1 molar equiv of nicotine, cotinine, pyridine, or *N*-methylpyrrolidine, was monitored over a 3-day period using centrifugation and ultraviolet spectroscopy. Over this period, nicotine and cotinine inhibited β-(1−42) precipitation,

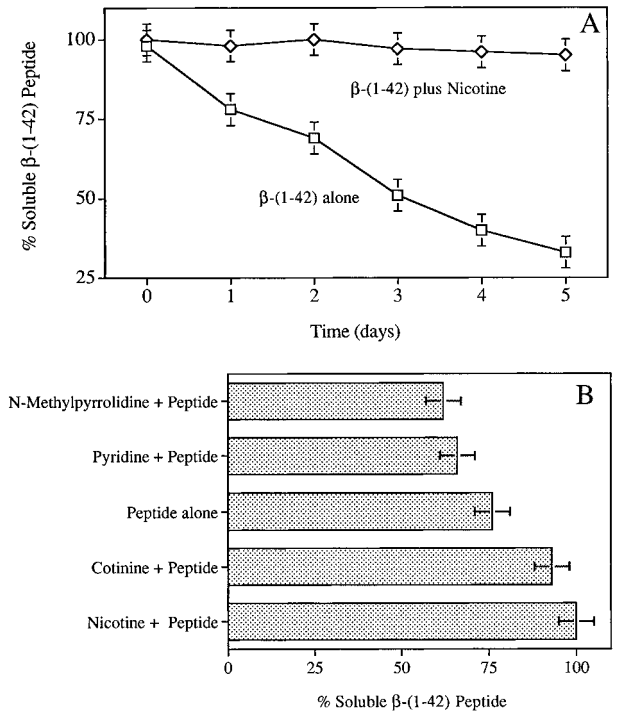

FIGURE 3: Graphs showing the effect of nicotine and control substances on the rate of β-(1−42) peptide precipitation as determined by ultraviolet spectroscopy. The concentrations of the β-(1−42) peptide, nicotine, cotinine, pyridine, and *N*-methylpyrrolidine were all 50 μM in buffered water solution at pH 7.2. As shown in the upper graph (A), nicotine completely inhibited precipitation for up to 5 days. The data in the lower graph (B) correspond to soluble β-(1−42) peptide remaining after 2 days.

with nicotine exerting a greater effect. However, both pyridine and *N*-methylpyrrolidine promoted precipitation (Figure 3B). These results suggest a possible structural requirement, in that both the pyrrolidine and pyridine ring moieties must be connected at the C3−C2′ bond to inhibit the β-(1−42) precipitation.

Nuclear Magnetic Resonance Binding Studies. To explore the possibility of nicotine binding to the β-peptide, we used 1D and 2D ^{1}H NMR spectroscopy. The solution NMR approach has the distinct advantage of being able to sequence-specifically locate individual amino acid side chains that bind to a particular ligand. However, it is not possible to obtain NMR spectra under the conditions used for the above CD and precipitation studies. In water solution, freshly dissolved monomeric β-(1−42) peptide is initially a mixture of rapidly interconverting α-helix, random coil, and aggregating β-sheet structures. This equilibrium would cause severe line broadening that would prevent the detection of resolved NMR signals. Additional line broadening would result from the subsequent aggregation and precipitation of the β-(1−42) peptide, particularly at the higher concentrations required for NMR spectroscopy.

Instead of using the β-(1−42) peptide, we used the shorter β-(1−28) peptide, which is amenable to NMR analysis (Figure 1). The β-(1−28) peptide is an appropriate structural model for the complete β-(1−42) peptide, since it produces soluble monomeric α-helical structures (Barrow & Zagorski, 1991; Otvos et al., 1993), as well as plaque-like oligomeric β-sheet structures, similar to those found in natural amyloid plaques (Gorévic et al., 1987; Kirschner et al., 1987). The hydrophobic 29−42 region increases the rate of aggregation and β-sheet production (Hilbich et al., 1991; Barrow et al., 1992; Burdick et al., 1992; Jarrett et al., 1993) but should not affect the ability of nicotine to bind to the β-peptide. Nicotine is a weak base with a pK_a of 7.9 (Jones, 1987), and at a blood pH of 7.4, nicotine is about 69% ionized and 31% un-ionized. Therefore, if binding does indeed occur, nicotine would be more likely to bind to the polar, hydrophilic 1−28 peptide region, rather than the completely hydrophobic 29−42 region (Figure 1).

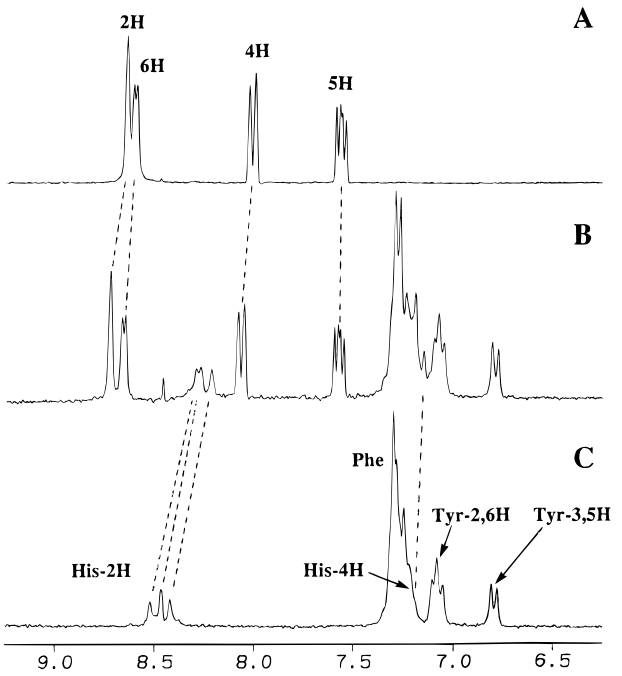

FIGURE 4: Downfield regions of the ^{1}H NMR spectra (270 MHz) for 10 mM nicotine (A) and 2 mM β-(1−28) peptide (C) in D_2O solution containing SDS-d_{25} (10 mM), pH 7.2 at 30.0 °C. The middle trace (B) is a spectrum of 4 mM nicotine and 2 mM β-(1−28) in SDS-d_{25} (10 mM) at pH 7.2. Assignments for the aromatic signals of nicotine (A) and the β-(1−28) peptide (C) are provided above the peaks. Those NMR peaks displaying chemical shift movements in the mixture (B) are connected to the original spectra (A and C) with dotted lines. The spectra represent 128 scans, digital resolution 0.24 Hz/pt, with the HDO signal suppressed by presaturation. All spectra are referenced to internal TSP.

For the present study, we first examined the possibility that nicotine binds to the α-helical structure of the 1−28 peptide region. An intriguing possibility is that nicotine may prevent the α-helix → β-sheet conversion, which occurs during aggregation, by binding and stabilizing the small amounts of α-helical structure that may be present for monomeric β-(1−42) peptide. The three-dimensional solution structure of the β-(1−28) peptide in trifluoroethanol/water and SDS-d_{25} micelle solution is predominantly α-helical (Talafous et al., 1994) and is qualitatively similar to that for the β-(1−40) peptide (Sticht et al., 1995). For the present study, we followed the binding of nicotine with the β-(1−28) peptide in SDS-d_{25} solution at pH 7.2. In SDS-d_{25} solution, the majority of the proton NMR resonances of the β-(1−28) peptide have been assigned (Talafous et al., 1994), and the NMR assignments for nicotine were obtained by 2D COSY.

Shown in Figure 4 are the downfield spectral regions of nicotine (Figure 4A), the β-(1−28) peptide with 2 molar equiv of nicotine (Figure 4B), and the β-(1−28) peptide alone (Figure 4C). The three, well-resolved histidine (His) 2H signals at 8.52, 8.47, and 8.42 ppm (Figure 4C) are consistent with the β-(1−28) peptide being folded into an ordered

Table 1: Chemical Shifts in the Complex of Nicotine and the β-(1−28) Peptide

NMR resonance	bound chemical shift (ppm)[a]	NMR resonance	bound chemical shift (ppm)[a]
peptide		nicotine	
His-2H	−0.22	2H′	0.07
His-4H	−0.06	5-α-CH′	0.24
nicotine		5-β-CH′	0.31
2H	0.10	$3CH_2'$	0.02
6H	0.07	$4CH_2'$	0.05
4H	0.07	N-CH_3	−0.50, 0.19
5H	0.03		

[a] Obtained by subtracting the chemical shifts in nicotine and the peptide from those seen in the complex. The negative shifts are upfield.

α-helical structure in SDS-d_{25} solution. If the predominate solution structure were random coil, then only one, degenerate His 2H signal would be present for His6, His13, and His14 (Zagorski & Barrow, 1992). The NMR spectrum of the 2:1 mixture of nicotine:β-(1−28) (Figure 2B) demonstrates that the peaks for nicotine and the His residues show changes in chemical shifts indicative of binding. The peptide His 2H and His 4H signals shift upfield 0.20 and 0.06 ppm, respectively, although the center His 2H signal at 8.47 ppm (Figure 4C), tentatively assigned to free or unbound His6, is still partly present in the mixture (Figure 4B). This suggests that nicotine may bind tighter to both His13 and His14 than to His6. Overall, the aromatic signals for the His residues are the only peaks showing any significant shift with nicotine. For example, the tyrosine and phenylalanine aromatic signals remain unperturbed with nicotine (Figure 4B), with the exception of minor 0.01 ppm upfield shifts of one phenylalanine signal (Figure 4B).

For nicotine most of the NMR signals undergo downfield chemical shifts in the presence of peptide. The aromatic 2H, 6H, 4H, and 5H pyridine ring protons shift downfield 0.10, 0.07, 0.07, and 0.03 ppm (Figure 4B), while the pyrrolidine $5'CH_2$ and N-CH_3 display larger downfield shifts of 0.24, 0.31, and 0.19 ppm (Figure 5B), respectively. For clarity, the upfield and downfield $5CH_2'$ protons at 3.07 and 3.64 ppm are named the 5-β-CH′ and 5-α-CH′ protons, respectively. Interestingly, the N-CH_3 displays two signals with peptide; one signal appears downfield by 0.19 ppm, while the second signal shifts upfield by 0.50 ppm. The two signals presumably represent two different orientations of the pyrrole ring when bound to the His residues of the peptide. A complete summary of the observed chemical shifts is shown in Table 1.

The NMR spectra shown in Figures 4 and 5 were obtained with a micelle−peptide ratio of 5, in which the SDS-d_{25} concentration was 10 mM, slightly above its critical micelle concentration of 8 mM (Henry & Sykes, 1994). Nearly identical chemical shifts were observed in spectra obtained with higher micelle−peptide ratios, and identical peptide α-helical CD spectra were observed at micelle concentrations below and above the aggregation number (Henry & Sykes, 1994). These data establish that the secondary structure of the peptide and the binding of the peptide to nicotine are not susceptible to the micelle concentration. In addition, with the exception of a slight reduction in the intensities of the His 2H signals, the spectrum of the peptide−nicotine mixture (Figure 5B) could be reproduced after allowing the solution to stand for 2 weeks at room temperature. The slight

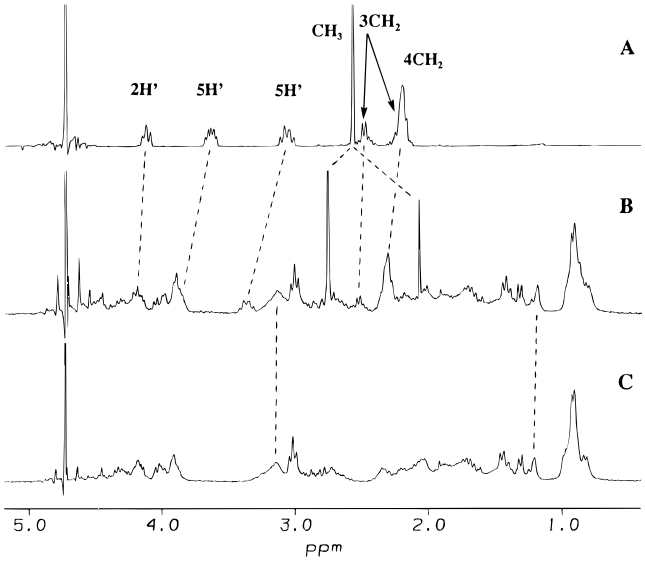

FIGURE 5: Upfield regions of the ^{1}H NMR spectra (270 MHz) for 10 mM nicotine (A) and 2 mM β-(1−28) peptide (C) in D_2O solution containing SDS-d_{25} (10 mM), pH 7.2 at 30.0 °C. The middle trace (B) is a spectrum of 4 mM nicotine and 2 mM β-(1−28) in SDS-d_{25} (10 mM) at pH 7.2. Assignments for the aliphatic signals of nicotine (A) are provided above the peaks. For clarity, in the text the upfield and downfield $5CH_2'$ protons at 3.07 and 3.64 ppm are referred to as 5-β-CH′ and 5-α-CH′, respectively. Those NMR peaks displaying chemical shift movements in the mixture (B) are connected to the original spectra (A and C) with dotted lines. The peak at 4.67 ppm corresponds to the remaining HDO signal that was suppressed by presaturation. All spectra are referenced to internal TSP.

reduction in the intensity of the His 2H signals results from hydrogen−deuterium exchange with the D_2O solvent.

To build upon the information provided by the 1D NMR studies, we next turned our attention to the 2D NOESY experiment. Expanded contour plots of the 2D NOESY spectra for nicotine, β-(1−28), and a 2:1 mixture in SDS-d_{25} solution obtained at 30 °C are shown in panels A−C of Figure 6, respectively. The 2D data were obtained in succession and processed using identical parameters. Due to the differences in molecular sizes and tumbling rates, the NOEs are negative for the peptide and positive for nicotine (Neuhaus & Williamson, 1989). The nicotine molecule is small and tumbles rapidly; thus the diagonal and cross peaks have opposite signs. This is shown in Figure 6A with red positive cross peaks and a black negative diagonal. In the NOESY spectra of the mixture (Figure 6C), the NOEs for nicotine become negative, consistent with the free nicotine becoming complexed to the peptide.

In the NOESY spectrum of nicotine (Figure 6A), the two, diastereotopic $5'CH_2$ protons show NOEs to each other and to the N-CH_3. There is also a weak NOE between the upfield 5′H and the $4'CH_2$. In the NOESY spectrum of the peptide alone (Figure 6B), the NOEs are analogous to spectra that we published earlier (Talafous et al., 1994), and the assignments of the Lys16 side chain resonances are shown along the diagonal. For the NOESY spectrum of the mixture (Figure 6C), other than the His residues, there are no apparent changes in chemical shifts for the peptide resonances, and new NOEs were not detected between the peptide and nicotine. However, the NMR resonances for nicotine shift in accordance with results seen in the 1D data (Figures 4B and 5B), and the NOE between the $5'CH_2$ and the N-CH_3 is now absent (Figure 6C). These results were established by

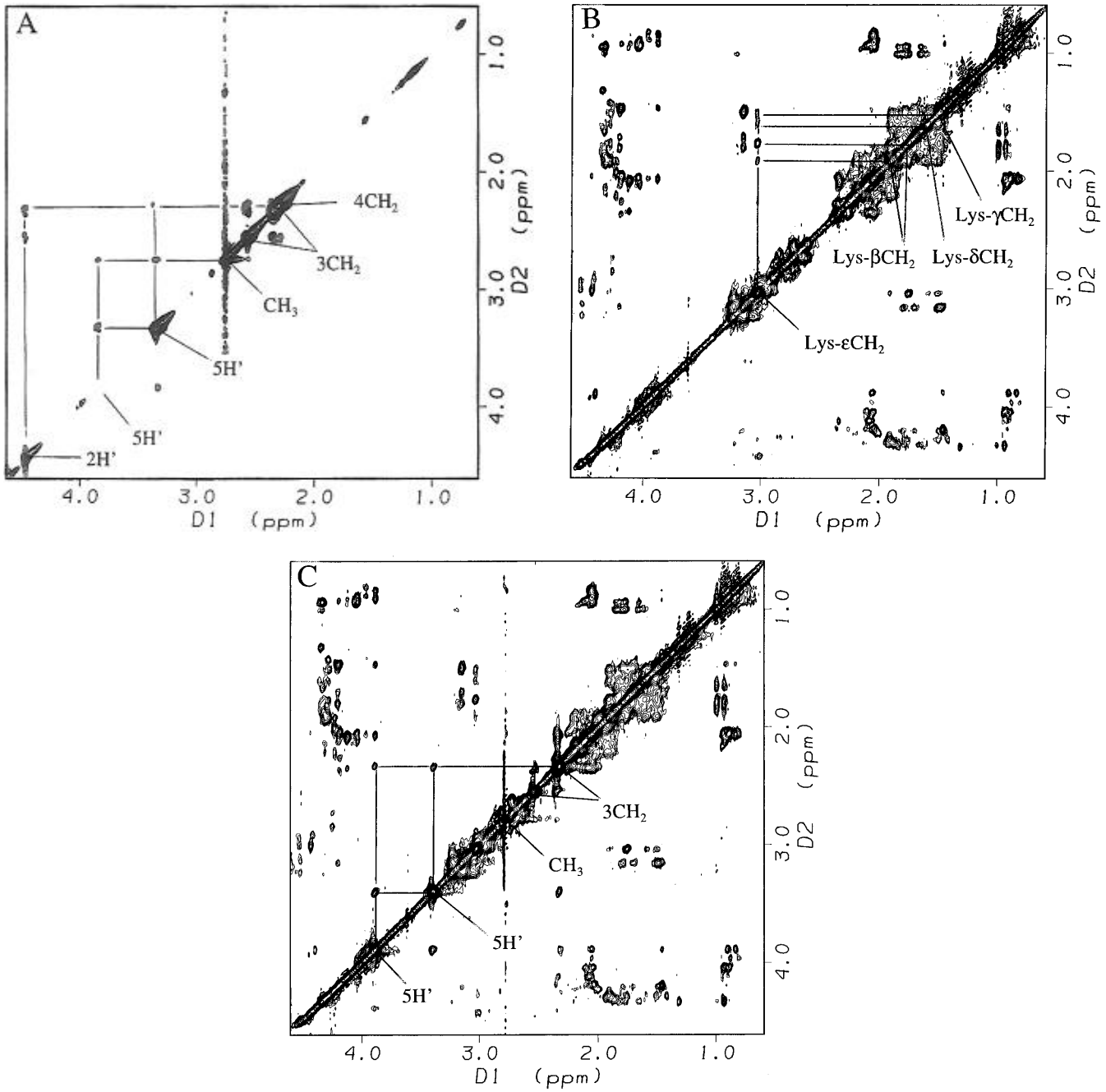

FIGURE 6: Upfield regions of phase-sensitive 2D NOESY spectra (600 MHz, mixing time 250 ms) for nicotine (10 mM) (A), β-(1−28) peptide (1.0 mM) (B), and the latter peptide solution with 2 molar equiv of nicotine (C). The data for the peptide only (B) and the 2:1 nicotine−peptide molar mixture (C) were obtained consecutively with identical parameters. The spectrum of nicotine alone (A) is plotted with positive (red) and negative (black) contours, demonstrating that the NOEs are all positive. The spectra of the peptide alone (B) and the peptide plus nicotine (C) contained only negative NOEs; thus the NOE cross peaks and the diagonal are the same phase. The assignments for the 5′CH_2 and the N-CH_3 of nicotine, together with the Arg5 and Lys16 side chains of the peptide, are shown. All samples were prepared in buffered D_2O solution containing 20 mM SDS-d_{25} at pH 7.2 and 30.0 °C. Chemical shifts are referenced to internal TSP.

overlaying NOESY spectra of free peptide (Figure 6B) with that of the mixture (Figure 6C). For all three NOESY experiments, spin diffusion was absent and only direct through-space interactions were detected (<5 Å), indicating that a 250 ms mixing time was appropriate for this study.

In summary, the chemical shift changes and the inversion in sign of the intramolecular NOEs for nicotine establish that nicotine binds to the His residues of the α-helix within residues 1−28 of the β-peptide. The lack of NMR resonances for free nicotine in the mixture is consistent with the binding being in the fast exchange range (Lian & Roberts, 1993).

DISCUSSION

Biological Functions of Nicotine and Its Relevance to Alzheimer's Disease. The purpose of the current study was to use well-established CD and NMR spectroscopic techniques to investigate the effects of nicotine and cotinine on the solution conformations and aggregational properties of the β-peptide. In the past our laboratory has used these methods for studies of the β-peptide [see Talafous et al. (1994) and references cited therein]. The results shown here establish that these methods can be successfully applied to investigate inhibitors of β-amyloidosis and their binding properties.

Nicotine in tobacco is hazardous to human health but in pure form has the potential to be a valuable pharmaceutical agent (Jones, 1987; Jarvick, 1991). Throughout the body, nicotine binds to the cholinergic nicotinic gating site on cationic ion channels in receptors, and this in turn causes the release of neurotransmitters such as catecholamines and serotonin. Repeated nicotine intake can promote positive reinforcement and enhancement of performance, together with protection against Parkinson's disease, Tourette's disease, ulcerative colitis, sleep apnea, and AD.

Because there are decreased levels of nicotinic receptors in AD brains, several investigations have examined the potential use of nicotine for treatment. The earliest studies utilized intravenous or subcutaneous administration (Newhouse et al., 1988; Sahakian et al., 1989; Jones et al., 1992). The results were generally positive with significant improvements in symptoms that are deficient in AD, including enhancement of immediate free recall, reaction time, and sustained visual attention. Subsequent studies showed that cigarette smoking, which contains high quantities of nicotine, reduces the risk of AD (Graves et al., 1991; Van Duijn & Hofman, 1991; Brenner et al., 1993; Friedland, 1994; Graves & Mortimer, 1994). It was also recently established that sustained transdermal-patch delivery of nicotine improved performances on learning tasks in AD patients (Wilson et al., 1995) and that nicotine reverses a β-(25−35) peptide induced amnesia in mice (Maurice et al., 1996). It is generally thought that the mechanism behind these beneficial effects is the upregulation of nicotine receptors that are deficient in AD brain.

The results shown here suggest that an alternative mechanism could account for the beneficial effects of nicotine in AD. This mechanism involves a nicotine inhibition to β-amyloidosis. A major weakness in this concept relates to the lack of physiological data to support a role for nicotine in amyloid formation or to support a role where nicotine binds to the amyloid β-peptide. Moreover, the conditions used in the present study were not performed at the reported physiological concentrations, so extrapolation of the results to humans is difficult. For smokers, the average concentration of nicotine in plasma is approximately 10−50 ng/mL (0.062−0.31 μM), which rises in the afternoon hours to 30−150 ng/mL (0.18−0.90 μM) (U. S. Department of Health and Human Services, 1988; Jones, 1987; Benowitz, 1990). The reported physiological concentrations of the β-peptide in cerebrospinal fluid of AD patients is 0.0033 ± 0.0014 μM, which is nearly identical to that of non-AD control patients (Southwick et al., 1996). For the present study, the lowest concentration we used was 3.1 μM, in which a nicotine inhibition to amyloidosis was seen, similar to the results at 50 μM. A more thorough analysis of the effects of varied concentrations of peptide and nicotine is clearly needed, and these studies are currently underway in our laboratory.

Our reasons for using higher, 50 μM concentrations is that the aggregation rate of the β-(1−42) peptide is too slow at lower concentrations. A 50 μM concentration is well suited for monitoring the rate of peptide precipitation and following the time-dependent conformational transition from random coil → β-sheet or α-helix → β-sheet by CD over several days. As mentioned before, this conformational transition appears to be an important factor to enhanced neurotoxicity of the β-peptide (Simmons et al., 1994; Harrigan et al., 1995; Pike et al., 1995). At normal, physiological concentrations the production of aggregated β-peptide as amyloid is very unlikely (Barrow et al., 1992; Jarrett & Lansbury, 1993; Snyder et al., 1994). The reported concentrations of β-(1−40) and β-(1−42) peptides in cerebrospinal fluid are well below the threshold concentrations (∼350 μM) required for rapid aggregation (Snyder et al., 1994). This suggests that, in order to produce amyloid deposits, localized regions of the brain must have much higher concentrations. The β-peptide concentrations in preamyloid deposits, which are likely precursors to the amyloid plaques, are possible candidates (Tagliavini et al., 1988; Yamaguchi et al., 1988; Wisniewski et al., 1994). Unlike the amyloid plaques, the preamyloid deposits show little neuritic alteration. It is generally thought that gradual, local accumulation of aggregated β-peptide into polymeric fibrils may be necessary for the preamyloid → amyloid plaque conversion in AD (Selkoe, 1994).

Structure and Relevance of the Nicotine/β-Peptide Binding. The relative predominance of a particular solution structure (α-helix, β-sheet, or random coil) of the β-peptide is strongly influenced by the conditions (Hilbich et al., 1991; Barrow et al., 1992; Burdick et al., 1992; Terzi et al., 1995). For solution NMR applications, it is necessary that the peptide adopts predominantly one defined structure, which is stable for long 2D NMR data acquisitions. Previous NMR studies demonstrated that the β-(1−28) peptide folds into an ordered α-helical structure at pH 1−4 and 7−10 in aqueous solutions containing trifluoroethanol or micelles (Zagorski & Barrow, 1992; Talafous et al., 1994). More recent NMR studies of a β-(10−35)-$CONH_2$ fragment suggest a turn−strand−turn motif between His13 and Val24 in aqueous solution (Lee et al., 1995), while the β-(1−40) peptide forms two α-helical segments between Gln15−Asp23 and Ile31−Met35 in aqueous trifluoroethanol solution (Sticht et al., 1995).

For the present study, we chose to investigate the binding of nicotine to the α-helical structure of the 1−28 region of the β-peptide. The α-helical structure is very soluble, amenable to NMR analysis, and easily forms in aqueous solution with SDS-d_{25} micelles (Talafous et al., 1994). It is not possible to study the β-(1−42) peptide in water solution at the higher concentrations required for NMR, since it adopts mixtures of rapidly interconverting α-helix, random coil, and aggregating β-sheet structures. This mixture of structures and the additional problem of peptide precipitation would prevent the detection of resolved NMR signals. Moreover, the 1−28 peptide region is the most relevant section for nicotine binding, since it is polar and charged at physiological pH. The charged nicotine molecule would be more likely to bind to the polar 1−28 peptide region instead of the nonpolar 29−42 region (Figure 1).

The NMR spectra for a 2:1 mixture of nicotine−peptide suggest that nicotine binds to the His residues of the α-helical structure (Figures 4 and 5). The identical 0.2 ppm upfield shift of the 2H for His6, His13, and His14 suggests that the binding mode between nicotine and all three His residues may be similar. The upfield shifts are interpreted in terms of ring-current shift contributions, with the His 2H situated above or below the pyridine aromatic ring of nicotine. The downfield chemical shifts seen for the pyrrolidine 5′CH_2 and N-CH_3 of nicotine indicate that this region interacts strongest with the peptide. In fact, all the nicotine NMR signals shift downfield, with the 5-α-CH′ and 5-β-CH′ signals having the

largest shifts of 0.24 and 0.31 ppm (Table 1). This deshielding was rationalized in terms of a ring-current contribution from the His aromatic rings (Perkins, 1982). The downfield shifts are consistent with 5′CH_2 protons located in the plane of the His rings.

Although the mixture contained a 1-fold excess of nicotine, NMR resonances for the free state of nicotine were not observed. The presence of single averaged resonances and the lack of any NOEs are consistent with nicotine binding to the peptide in a fast exchange manner (Lian & Roberts, 1993). If the binding was in slow exchange, then two separate NMR resonances for the free and bound states would be present. A more complete analysis of the binding exchange rates and the determination of a binding constant will require additional studies with a wider range of peptide and nicotine concentrations.

Mechanism of the Nicotine Inhibition to Amyloidosis. The neuropathological hallmarks of AD brains are the abundance of intraneuronal neurofibrillary tangles and the deposition of the β-peptide in the form of amyloid plaques. Additionally, the degree of neuronal damage and dementia in AD correlates with the extent of neurofibrillary tangle and amyloid plaque formation (Perry et al., 1978; Selkoe, 1994). Several lines of evidence suggest that free-radical-based oxidative damage by the β-peptide is responsible for the neurodegeneration in AD (Harris et al., 1995; Schubert et al., 1995; Goodman & Mattson, 1996). Other data suggest that the neurotoxicity is directly related to the β-peptide aggregation state and its propensity to generate β-sheet secondary structures (Simmons et al., 1994; Harrigan et al., 1995; Pike et al., 1995). More recent data suggest that fibrillar β-peptide and focal amyloid deposits are not neurotoxic and that more soluble, partly aggregated complexes cause neurotoxicity (Oda et al., 1995; Wujek et al., 1996). It may happen that the aggregation, secondary structure, and production of free radical species all play a role in β-peptide-induced neurotoxicity. However, since nearly identical quantities of soluble β-peptide are found in AD and age-matched-control patients (Southwick et al., 1996), it seems more likely that generation of the amyloid plaques that contain aggregated β-sheet structure is pivotal to the neurotoxicity.

Despite over a decade of research, the underlying mechanisms of the β-peptide-induced neurotoxicity and its accumulation into insoluble amyloid deposits remain unknown. The most widely accepted concept involves an "amyloid-initiated-cascade" phenomenon, where altered production, removal, and aggregation of the amyloid β-peptide initiates a sequence of events that leads to neuronal death (Wisniewski et al., 1994; Selkoe, 1995). The amyloidosis may occur by the attachment of the β-peptide to larger macromolecules, metals, or small amounts of preaggregated peptide that can act as a seed for precipitation. Some of the other components that induce aggregation include glycosaminoglycans (Brunden et al., 1993), zinc (Mantyh et al., 1993; Bush et al., 1994), apolipoprotein-E (Strittmatter et al., 1993; Ma et al., 1994; Evans et al., 1995; Soto et al., 1995c), glycation (Smith et al., 1994; Vitek et al., 1994), or NACP (Yoshimoto et al., 1995). A list of the components that promote or retard aggregation and toxicity of the β-peptide is given in Iversen et al. (1995).

We and others have proposed another more detailed concept (Barrow et al., 1992; Talafous et al., 1994; Soto et al., 1995a; Soto & Frangione, 1995), in which amyloidosis of the β-peptide involves a conformationally driven mechanism, with soluble monomeric α-helical structures producing oligomeric β-sheet structures that are toxic to neurons. Related α-helix → β-sheet conversions for other peptides and proteins (Fan et al., 1993; Graf v. Stosch et al., 1995), including peptide segments of the prion proteins (Nguyen et al., 1995; Zhang et al., 1995) are well documented. These processes occur during normal aging that can be accompanied by changes of brain microenvironments, including β-peptide concentrations, pH, and membrane integrity. These environmental factors can accelerate amyloid plaque formation and prevent proteolysis of the β-peptide in AD. In the amyloid plaque, the β-peptide exists in an oligomeric β-pleated sheet structure that is resistant to further proteolysis and turnover (Crowther, 1991; Nordstedt et al., 1994). It may happen that the soluble β-sheet structure, which forms before the plaque, is likewise resistant to proteolysis, similar to soluble peptide segments of the amyloid forming prion proteins (Zhang et al., 1995).

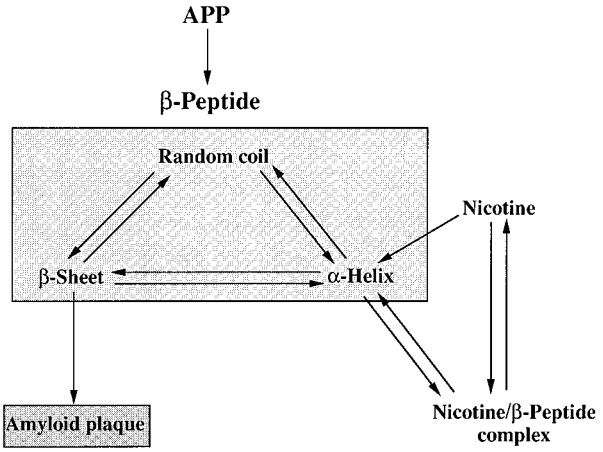

FIGURE 7: Mechanism of nicotine inhibition to amyloidosis, where nicotine prevents β-sheet formation by binding to the monomeric α-helical structure. Once generated by proteolytic cleavage from the amyloid precursor protein (APP) (Selkoe, 1994), the β-peptide is soluble and adopts an equilibrium mixture of random coil, monomeric α-helix, and oligomeric β-sheet structures. When the β-sheet structure reaches a critical mass, it precipitates as an amyloid deposit, and this causes the equilibrium to shift toward more β-sheet structure. Inhibitors of amyloidosis, such as nicotine, would bind to the more soluble α-helical structure and slow down or prevent an α-helix → β-sheet conversion.

The present study establishes that nicotine binds to the α-helical structure within residues 1−28 of the β-peptide, which provides a rationale for the nicotine inhibition to β-sheet production and precipitation. As outlined in Figure 7, the binding may slow down or prevent an α-helix → β-sheet conversion. In solution, freshly prepared, monomeric β-(1−42) peptide adopts mixtures of α-helix, random coil, and β-sheet structures that are in equilibrium. The precipitation drives the equilibrium toward β-sheet structure, so once precipitation has begun the α-helical structure will rearrange to the oligomeric β-sheet structure [α-helix → β-sheet (solution) → β-sheet (precipitate)]. For the peptide solutions with and without nicotine, at 0 h the respective CD data showed 8% and 58% β-sheet structure (Figure 2C). The small amount of β-sheet structure for the solution containing nicotine, along with the absence of an isodichroic point in the CD spectra (Figure 2B), suggests that initially greater than two conformations coexist in solution. The weak

negative band at 195 nm establishes that the major conformation is random coil (Figure 2B), but it is conceivable that minor quantities of α-helical structures may be present. In support of this notion, recent molecular dynamics simulations in water solution at physiological pH showed that the β-(1−28) peptide adopts a rapidly interconverting ensemble of conformations, with significant quantities of α-helical structure (Kirshenbaum & Daggett, 1995). Although our previous CD studies indicate that the β-(1−28) adopts predominantly random coil structure in water solution at physiological pH (Barrow et al., 1992), Kirshenbaum and Daggett (1995) suggested that the α-helical CD bands may be diminished due to the presence of large quantities of unfolded species. This explanation supports the conclusions in the present study.

CONCLUSIONS

Detailed knowledge of the chemistry, solution structures, and molecular mechanisms of amyloidosis of the β-peptide is urgently needed, since they can guide parallel pharmacological studies. On the basis of results from CD and NMR, we first proposed (Barrow & Zagorski, 1991) that the β-peptide may *normally* exist in human biological fluids in a soluble form and that the longer 42-residue peptide results from an abnormal proteolysis. Subsequently, both of our propositions were shown to be correct using both in vivo and in vitro studies (Seubert et al., 1992; Shoji et al., 1992; Busciglio et al., 1993; Suzuki et al., 1994). There are currently no effective treatments for AD, and the current drug development process is often cumbersome, taking an average 8.8 years for approval (Cutler & Sramek, 1995). The present study represents the first example of the combined use of a standard precipitation assay, together with CD and NMR techniques to study the interaction of a small organic molecule with the amyloid β-peptide. This work established that in vitro nicotine and cotinine inhibit amyloidosis, perhaps by binding to the more soluble α-helical structure and preventing an α-helix → β-sheet conversion. This approach can assist in the design of less toxic analogs to prevent an α-helix → β-sheet conversion during amyloidosis in AD, which may be applied to treatment of the disease. Most significantly, recent studies showed that nicotine inhibits β-peptide-induced neurotoxicity (Kihara et al., 1996; Shimohama, 1996). Although it is not yet known whether in vivo nicotine inhibits amyloidosis, the work presented here suggests that further research into this possibility would be a worthwhile endeavor.

ACKNOWLEDGMENT

The authors thank Thomas Lentz, Mark Smith, Lawrence Sayre, and Dave McCoy for many thoughtful discussions and Robert Salomon for the use of his centrifuge.

REFERENCES

Barrow, C. J., & Zagorski, M. G. (1991) *Science 253*, 179−182.

Barrow, C. J., Yasuda, A., Kenny, P. T. M., & Zagorski, M. G. (1992) *J. Mol. Biol. 225*, 1075−1093.

Benowitz, N. L. (1990) *Pharmacokinetic Considerations in Understanding Nicotine Dependence*, John Wiley and Sons, New York.

Brenner, D., Kukull, W., van Belle, G., Bowen, J., McCormick, W., Teri, L., & Larson, E. (1993) *Neurology 43*, 293−300.

Brunden, K. R., Richter-Cook, N. J., Chaturvedi, N., & Frederickson, R. C. A. (1993) *J. Neurochem. 61*, 2147−2154.

Burdick, D., Soreghan, B., Kwon, M., Kosmoski, J., Knauer, M., Henschen, A., Yates, J., Cotman, C., & Glabe, C. (1992) *J. Biol. Chem. 267*, 546−554.

Busciglio, J., Lorenzo, A., & Yanker, B. A. (1992) *Neurobiol. Aging 13*, 609−612.

Busciglio, J., Gabuzda, D. H., Matsudaira, P., & Yanker, B. A. (1993) *Proc. Natl. Acad. Sci. U.S.A. 90*, 2092−2096.

Bush, A. I., Pettingell, W. H., Multhaup, G., Paradis, M., Vonsattel, J.-P., Gusella, J. F., Beyreuther, K., Masters, C. L., & Tanzi, R. E. (1994) *Science 265*, 1464−1467.

Cantor, C. R., & Schimmel, P. R. (1980) *Biophysical Chemistry: Part I, The Conformation of Biological Macromolecules*, W. H. Freeman, New York.

Crowther, R. A. (1991) *Biochim. Biophys. Acta 1096*, 1−9.

Cutler, N. R., & Sramek, J. J. (1995) *Drug Development Must be Optimized in Order to Choose the Correct Strategy*, Wiley, New York.

Eriksson, S., Janciauskiene, S., & Lannfelt, L. (1995) *Proc. Natl. Acad. Sci. U.S.A. 92*, 2313−2317.

Esler, W. P., Stimson, E. R., Jennings, J. M., Ghilardi, J. R., Mantyh, P. W., & Maggio, J. E. (1996) *J. Neurochem. 66*, 723−732.

Evans, K. C., Berger, E. P., Cho, C.-G., Weisgraber, K. H., & Lansbury, P. T. (1995) *Proc. Natl. Acad. Sci. U.S.A. 92*, 763−767.

Fan, P., Bracken, C., & Baum, J. (1993) *Biochemistry 32*, 1573−1582.

Fraser, P. E., Nguyen, J. T., Surewicz, W. K., & Kirschner, D. A. (1991) *Biophys. J. 60*, 1190−1201.

Friedland, R. P. (1994) *Neurobiol. Aging 15*, 239−241.

Goodman, Y., & Mattson, M. P. (1996) *J. Neurochem. 66*, 869−872.

Gorévic, P. D., Castano, E. M., Sarma, R., & Frangione, B. (1987) *Biochem. Biophys. Res. Commun. 147*, 854−862.

Graf v. Stosch, A., Jiménez, M. A., Kinzel, V., & Reed, J. (1995) *Proteins 23*, 196−203.

Graves, A. B., & Mortimer, J. A. (1994) *J. Smoking-Related Disord. 5*, 79−90.

Graves, A. B., van Duijn, C. M., Chandra, V., Fratiglioni, L., Heyman, A., Jorm, A. F., et al. (1991) *Int. J. Epidemiol. 20* (Suppl 2), S48−S57.

Gravina, S. A., Ho, L., Eckman, C. B., Long, K. E., Laszlo Otvos, J., Younkin, L. H., Suzuki, N., & Younkin, S. G. (1995) *J. Biol. Chem. 270*, 7013−7016.

Greenfield, N., & Fasman, G. D. (1969) *Biochemistry 8*, 4108−4116.

Harrigan, M. R., Kunkel, D. D., Nguyen, L. B., & Malouf, A. T. (1995) *Neurobiol. Aging 16*, 779−789.

Harris, M. E., Hensley, K., Butterfield, D. A., Leedle, R. A., & Carney, J. M. (1995) *Exp. Neurol. 131*, 193−202.

Henry, G. D., & Sykes, B. D. (1994) *Methods Enzymol. 239*, 520−534.

Hilbich, C., Kisters-Woide, B., Reed, J., Masters, C. L., & Beyreuther, K. (1991) *J. Mol. Biol. 218*, 149−163.

Iversen, L. L., Mortishire-Smith, R. J., Pollack, S. J., & Shearman, M. S. (1995) *Biochem. J. 311*, 1−16.

Janciauskiene, S., Frutos, P. G. d., Carlemalm, E., Dahlbäck, B., & Eriksson, S. (1995) *J. Biol. Chem. 270*, 26041−26044.

Jarrett, J. T., & Lansbury, P. T. J. (1993) *Cell 73*, 1055−1058.

Jarrett, J. T., Beger, E. P., & Lansbury, P. T. J. (1993) *Biochemistry 32*, 4693−4697.

Jarvick, M. E. (1991) *Br. J. Addict. 86*, 571−575.

Jones, G. M., Sahakian, B. J., Levy, R., Warburton, D. M., & Gray, J. (1992) *Psychopharmacology 108*, 485−494.

Jones, R. T. (1987) *Tobacco Dependence*, Raven Press, New York.

Kihara, T., Shimohama, S., Sawada, H., Kimura, J., Kume, T., Maeda, T., & Akaike, A. (1996) *Neurobiol. Aging 17*, S429.

Kirschner, D. A., Inouye, H., Duffy, L. K., Sinclair, A., Lind, M., & Selkoe, D. J. (1987) *Proc. Natl. Acad. Sci. U.S.A. 84*, 6953−6957.

Kirshenbaum, K., & Daggett, V. (1995) *Biochemistry 34*, 7629−7639.

Kumar, A., Ernst, R. R., & Wüthrich, K. (1980) *Biochem. Biophys. Res. Commun. 95*, 1−6.

Lee, J. P., Stimson, E. R., Ghilardi, J. R., Mantyh, P. W., Lu, Y.-A., Felix, A. M., Llanos, W., Behbin, A., Cummings, M., van Criekinge, M., Timms, W., & Maggio, J. E. (1995) *Biochemistry 34*, 5191−5200.

Lian, L.-Y., & Roberts, G. C. K. (1993) *Effects of Chemical Exchange on NMR Spectra*, Oxford University Press, Oxford.

Lide, D. R. (1991) *CRC Handbook of Chemistry and Physics*, 71st ed., CRC Press, Boca Raton, FL.

Ma, J., Yee, A., Brewer, H. B. J., Das, S., & Potter, H. (1994) *Nature 372*, 92−94.

Mantyh, P. W., Ghilardi, J. R., Rogers, S., DeMaster, E., Allen, C. J., Stimson, E. R., & Maggio, J. E. (1993) *J. Neurochem. 61*, 1171−1174.

Maurice, T., Lockhart, B. P., & Privat, A. (1996) *Brain Res. 706*, 181−193.

Neuhaus, D., & Williamson, M. P. (1989) *The Nuclear Overhauser Effect in Structural and Conformational Analysis*, VCH Publishers, New York.

Newhouse, P. A., Sunderland, T., Tariot, P. N., Blumhardt, C. L., Weingartner, H., Mellow, A., & Murphy, D. L. (1988) *Psychopharmacology 95*, 171−175.

Nguyen, J., Baldwin, M. A., Cohen, F. E., & Prusiner, S. B. (1995) *Biochemistry 34*, 4186−4192.

Nordstedt, C., Näslund, J., Tjernberg, L. O., Karlström, A. R., Thyberg, J., & Terenius, L. (1994) *J. Biol. Chem. 269*, 30773−30776.

Oda, T., Wals, P., Osterburg, H. H., Johnson, S. A., Pasinetti, G. M., Morgan, T. E., Rozovsky, I., Stine, W. B., Snyder, S. W., Holzman, T. F., Krafft, G. A., & Finch, C. E. (1995) *Exp. Neurol. 136*, 22−31.

Otting, G., Widmer, H., Wagner, G., & Wüthrich, K. (1986) *J. Magn. Reson. 66*, 187−193.

Otvos, L. J., Szendrei, G. I., Lee, V. M. Y., & Mantsch, H. H. (1993) *Eur. J. Biochem. 211*, 249−257.

Perkins, S. J. (1982) *Applications of Ring Current Calculations to the Proton NMR of Proteins and Transfer RNA*, Plenum Press, New York.

Perry, E. K., Tomlinson, B. E., Blessed, G., Bergman, K., Gibson, P. H., & Perry, R. H. (1978) *Br. Med. J. 2*, 1457−1459.

Pike, C. J., Burdick, D., Walencewicz, A. J., Glabe, C. G., & Cotman, C. W. (1993) *J. Neurosci. 13*, 1676−1687.

Pike, C. J., Walencewicz-Wasserman, A. J., Kosmoski, J., Cribbs, D. H., Glabe, C. G., & Cotman, C. W. (1995) *J. Neurochem. 64*, 253−265.

Roher, A. E., Lowenson, J. D., Clarke, S., Woods, A. S., Cotter, R. J., Gowing, E., & Ball, M. J. (1993) *Proc. Natl. Acad. Sci. U.S.A. 90*, 10836−10840.

Sahakian, B., Jones, G., Levy, R., Gray, J., & Warburton, D. (1989) *Br. J. Psychiatry 154*, 797−800.

Schubert, D., Behl, C., Lesley, R., Brack, A., Dargusch, R., Sagara, Y., & Kimura, H. (1995) *Proc. Natl. Acad. Sci. U.S.A. 92*, 1989−1993.

Selkoe, D. J. (1994) *Annu. Rev. Neurosci. 17*, 489−517.

Selkoe, D. J. (1995) *J. NIH Res. 7*, 57−64.

Seubert, P., Vigo-Pelfrey, C., Esch, F., Lee, M., Dovey, H., Davis, D., Sinha, S., Schlossmacher, M., Whaley, J., Swindlehurst, C., McCormack, R., Wolfert, R., Selkoe, L., I., & Schenk, D. (1992) *Nature 359*, 325−327.

Shen, C.-L., & Murphy, R. M. (1995) *Biophys. J. 69*, 640−651.

Shen, C.-L., Fitzgerald, M. C., & Murphy, R. M. (1994) *Biophys. J. 67*, 1238−1246.

Shimohama, S. (1996) *Neurobiol. Aging 17*, S40.

Shoji, M., Golde, T. E., Cheung, T. T., Ghiso, J., Estus, S., & Shaffer, L. M. (1992) *Science 258*, 126−129.

Simmons, L. K., May, P. C., Tomaselli, K. J., Rydel, R. E., Fuson, K. S., Brigham, E. F., Wright, S., Lieberburg, I., Becker, G. W., Brems, D. N., & Li, W. (1994) *Mol. Pharmacol. 45*, 373−379.

Smith, M. A., Taneda, S., Richey, P. L., Miyata, S., Yan, S.-D., Stern, D., Sayre, L. M., Monnier, V. M., & Perry, G. (1994) *Proc. Natl. Acad. Sci. U.S.A. 91*, 5710−5714.

Snyder, S. W., Ladror, U. S., Wade, W. S., Wang, G. T., Barrett, L. W., Matayoshi, E. D., Huffaker, H. J., Krafft, G. A., & Holzman, T. F. (1994) *Biophys. J. 67*, 1216−1228.

Soto, C., & Frangione, B. (1995) *Neurosci. Lett. 186*, 115−118.

Soto, C., Castano, E. M., Frangione, B., & Inestrosa, N. C. (1995a) *J. Biol. Chem. 270*, 3063−3067.

Soto, C., Castaño, E. M., Kumar, R. A., Beavis, R. C., & Frangione, B. (1995b) *Neurosci. Lett. 200*, 105−108.

Soto, C., Castaño, E. M., Prelli, F., Kumar, R. A., & Baumann, M. (1995c) *FEBS Lett. 371*, 110−114.

Southwick, P. C., Yamagata, S. K., Echols, C. L., Higson, G. J., Neynaber, S. A., Parson, R. E., & Munroe, W. A. (1996) *J. Neurochem. 66*, 259−265.

States, D. J., Haberkorn, R. A., & Ruben, D. J. (1982) *J. Magn. Reson. 48*, 286−292.

Sticht, H., Bayer, P., Willbold, D., Dames, S., Hilbich, C., Beyreuther, K., Frank, R. W., & Rösch, P. (1995) *Eur. J. Biochem. 233*, 293−298.

Strittmatter, W. J., Weisgraber, K. H., Huang, D. Y., Dong, L.-M., Salvesen, G. S., Pericak-Vance, M., Schmechel, D., Saunders, A. M., Goldgabr, D., & Roses, A. D. (1993) *Proc. Natl. Acad. Sci. U.S.A. 90*, 8098−8102.

Suzuki, N., Cheung, T. T., Cai, X.-D., Odaka, A., Otvos, L., Eckman, C., Golde, T. E., & Younkin, S. G. (1994) *Science 264*, 1336−1340.

Tagliavini, F., Giaccone, G., Frangione, B., & Bugiani, O. (1988) *Neurosci. Lett. 93*, 191−196.

Talafous, J., Marcinowski, K. J., Klopman, G., & Zagorski, M. G. (1994) *Biochemistry 33*, 7788−7796.

Tamaoka, A., Kondo, T., Odaka, A., Sahara, N., Sawamura, N., Ozawa, K., Suzuki, N., Shoji, S., & Mori, H. (1994) *Biochem. Biophys. Res. Commun. 205*, 834−842.

Terzi, E., Hölzemann, G., & Seelig, J. (1994) *Biochemistry 33*, 1345−1350.

Terzi, E., Hölzemann, G., & Seelig, J. (1995) *J. Mol. Biol. 252*, 633−642.

U.S. Department of Health and Human Services (1988) *A Report of the Surgen General*, Rockville, MD.

Van Duijn, C., & Hofman, A. (1991) *Br. Med. J. 302*, 1491−1494.

Vitek, M. P., Bhattacharya, K., Glendening, J. M., Stopa, E., Vlassara, H., Bucala, R., Manogue, K., & Cerami, A. (1994) *Proc. Natl. Acad. Sci. U.S.A. 91*, 4766−4770.

Wilson, A. L., McCarten, J. R., Langley, L. K., Bauer, T., Monley, J., Rottunda, S., McFalls, E., & Kovera, C. (1995) *Transdermal Nicotine Administration in Alzheimer's Disease: Effects on Cognition, Behavior, and Cardiac Function*, Wiley, New York.

Wisniewski, T., Ghiso, J., & Frangione, B. (1994) *Neurobiol. Aging 15*, 143−152.

Wood, S. J., MacKenzie, L., Maleef, B., Hurle, M. R., & Wetzel, R. (1996) *J. Biol. Chem. 271*, 4086−4092.

Wujek, J. R., Dority, M. D., Frederickson, R. C. A., & Brunden, K. R. (1996) *Neurobiol. Aging 17*, 107−113.

Wüthrich, K. (1986) *NMR of Proteins and Nucleic Acids*, Wiley, New York.

Yamaguchi, H., Hirai, S., Morimatsu, M., Shoji, M., & Harigaya, Y. (1988) *Acta Neuropathol. 77*, 113−119.

Yoshimoto, M., Iwai, A., Kang, D., Otero, D. A. C., Xia, Y., & Saitoh, T. (1995) *Proc. Natl. Acad. Sci. U.S.A. 92*, 9141−9145.

Zagorski, M. G., & Barrow, C. J. (1992) *Biochemistry 31*, 5621−5631.

Zhang, H., Kaneko, K., Nguyen, J. T., Livshits, T. L., Baldwin, M. A., Cohen, F. E., James, T., & Prusiner, S. B. (1995) *J. Mol. Biol. 250*, 514−526.

BI9617264